

The Dual Gonihedric 3D Ising Model

D. A. Johnston

Dept. of Mathematics, Heriot-Watt University, Riccarton, Edinburgh, EH14 4AS,
Scotland

R. P. K. C. M. Ranasinghe

Department of Mathematics, University of Sri Jayewardenepura, Gangodawila, Sri
Lanka.

Abstract.

We investigate the dual of the $\kappa = 0$ Gonihedric Ising model on a $3D$ cubic lattice, which may be written as an anisotropically coupled Ashkin-Teller model. The original $\kappa = 0$ Gonihedric model has a purely plaquette interaction, displays a first order transition and possesses a highly degenerate ground state.

We find that the dual model admits a similar large ground state degeneracy as a result of the anisotropic couplings and investigate the coupled mean field equations for the model on a single cube. We also carry out Monte Carlo simulations which confirm a first order phase transition in the model and suggest that the ground state degeneracy persists throughout the low temperature phase. Some exploratory cooling simulations also hint at non-trivial dynamical behaviour.

1. Introduction

The Gonihedric Ising model has an interesting history, having originally been formulated as a fixed lattice version of a discretized string/triangulated random surface action suggested by Savvidy *et.al.*, whose action was given by [1]

$$S = \frac{1}{2} \sum_{\langle ij \rangle} |\vec{X}_i - \vec{X}_j| \theta(\alpha_{ij}), \quad (1)$$

where $\theta(\alpha_{ij}) = |\pi - \alpha_{ij}|$ and α_{ij} is the dihedral angle between the embedded neighbouring triangles with a common link $\langle ij \rangle$. The $|\vec{X}_i - \vec{X}_j|$ are the lengths of the embedded triangle edges as shown in Fig. (1). The aim of this action was to weight the edges of non-coplanar adjoining triangles on a discretized surface, rather than the triangle areas as is the case with a Gaussian action, in an attempt to search for a continuum limit which might be related to a string theory. The discretized random surfaces formed from gluing together triangles were intended to model Euclidean string worldsheets.

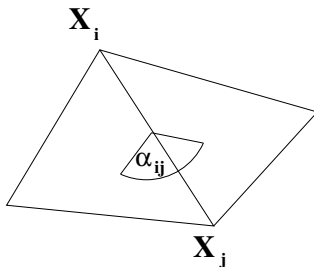


Figure 1. Two adjacent triangles in a triangulation of a surface with a common edge $\langle ij \rangle$, showing the co-ordinates of the endpoints $\vec{X}_{i,j}$ and the dihedral angle α_{ij}

Translating this action onto a fixed cubic lattice and asking that the requisite surfaces be represented by the plaquettes of spin cluster boundaries in some Ising-like model trivializes the edge length $|\vec{X}_i - \vec{X}_j|$ dependence, so the statistical weights of surface configurations depend solely on the $\theta(\alpha_{ij}) = |\pi - \alpha_{ij}|$ factors, where the α_{ij} are now restricted to multiples of $\pi/2$ radians. The statistical weights of such plaquette surface configurations will be determined entirely by the number of bends and self-intersections they contain.

The mapping between the energies of a gas of plaquette surfaces and generalised Ising models was studied in some detail by Cappi *et.al.* [2] who calculated the energies of spin cluster boundaries on the 3D cubic lattice for an Ising spin (± 1) Hamiltonian which contains nearest neighbour $\langle i, j \rangle$, next to nearest neighbour $\langle\langle i, j \rangle\rangle$ and plaquette $[i, j, k, l]$ terms

$$-\beta H = J_1 \sum_{\langle ij \rangle} \sigma_i \sigma_j + J_2 \sum_{\langle\langle i, j \rangle\rangle} \sigma_i \sigma_j + J_3 \sum_{[i, j, k, l]} \sigma_i \sigma_j \sigma_k \sigma_l. \quad (2)$$

The couplings in such models can be related to the couplings for the area energy of plaquettes in spin cluster boundaries, β_A , the energy cost of a right-angled bend between

two such adjacent plaquettes, β_C , and the energy cost, β_I , for the intersection of four plaquettes having a link in common

$$\begin{aligned}\beta_A &= 2J_1 + 8J_2 \\ \beta_C &= 2J_3 - 2J_2 \\ \beta_I &= -4J_2 - 4J_3.\end{aligned}\tag{3}$$

The original 3D Gonihedric model [3] constitutes a particular one-parameter slice of this family of Hamiltonians:

$$H = -2\kappa \sum_{\langle ij \rangle} \sigma_i \sigma_j + \frac{\kappa}{2} \sum_{\langle\langle ij \rangle\rangle} \sigma_i \sigma_j - \frac{1-\kappa}{2} \sum_{[i,j,k,l]} \sigma_i \sigma_j \sigma_k \sigma_l.\tag{4}$$

For this ratio of couplings $\beta_A = 0$, which means that the edges and intersections of spin cluster boundaries are weighted rather than their area, which is the antithesis of the usual 3D Ising model with only nearest neighbour spin interactions where $\beta_I = \beta_C = 0$. The energy of the spin cluster boundaries for the Gonihedric model on a cubic lattice is simply given by $E = n_2 + 4\kappa n_4$, where n_2 is the number of links where two plaquettes on a spin cluster boundary meet at a right angle, n_4 is the number of links where four plaquettes meet at right angles and κ is the free parameter. It is worth remarking that the language we have employed implicitly assumes that spin cluster boundaries can be clearly identified. As we shall see below this may not be such a simple matter for the dual Gonihedric model (it is similarly complicated for the original Gonihedric action, at least when $\kappa = 0$).

When $\kappa = 0$ the Gonihedric Hamiltonian becomes a purely plaquette term

$$H = -\frac{1}{2} \sum_{[i,j,k,l]} \sigma_i \sigma_j \sigma_k \sigma_l\tag{5}$$

which is *not* the 3D gauge Ising model, since the spins live on the vertices rather than the edges of the lattice. This plaquette action displays a first order transition surrounded by a region of metastability [4]. It also displays interesting dynamical behaviour with a dynamical transition at the lower boundary of the metastable region which appears to have many glassy characteristics [5–8]. This is intriguing because there is no quenched disorder in the Hamiltonian.

The dual to the $\kappa = 0$ Gonihedric Ising model was constructed by Savvidy and Wegner [9]. They considered a high temperature expansion of the partition function for the Hamiltonian in equ.(5)

$$\begin{aligned}Z(\beta) &= \sum_{\{\sigma\}} \exp(-\beta H) \\ &= \sum_{\{\sigma\}} \prod_{[i,j,k,l]} \cosh\left(\frac{\beta}{2}\right) \left[1 + \tanh\left(\frac{\beta}{2}\right) (\sigma_i \sigma_j \sigma_k \sigma_l)\right]\end{aligned}\tag{6}$$

which can be written as

$$Z(\beta) = \left[2 \cosh\left(\frac{\beta}{2}\right)\right]^{3L^3} \sum_{\{S\}} \left[\tanh\left(\frac{\beta}{2}\right)\right]^{n(S)}\tag{7}$$

on an L^3 cubic lattice. The sum runs over closed surfaces with an even number of plaquettes at any vertex and $n(S)$ is the number of plaquettes in a given surface. This ensemble can be constructed from three differently oriented elementary “matchbox” surfaces of the form shown in Fig. (2) along with the unshaded cube. A spin variable representing each matchbox then sits at the centre of the cube on the dual lattice and any surface in the ensemble can be constructed as a product of the elementary matchboxes and unshaded cubes. When two shaded matchbox faces overlap they annihilate to give an unshaded face, so the shaded faces can be thought of as carrying a negative sign.

The low temperature expansion of the dual Hamiltonian

$$H_{dual} = -\frac{1}{2} \sum_{\langle ij \rangle} \sigma_i \sigma_j - \frac{1}{2} \sum_{\langle ik \rangle} \tau_i \tau_k - \frac{1}{2} \sum_{\langle jk \rangle} \eta_j \eta_k \quad (8)$$

gives precisely this structure, where σ, τ and η represent each of the possible matchbox orientations. In equ.(8) the spins σ, τ and η live on the vertices of the dual lattice and the sums are along its orthogonal edges ij, ik and jk . They satisfy

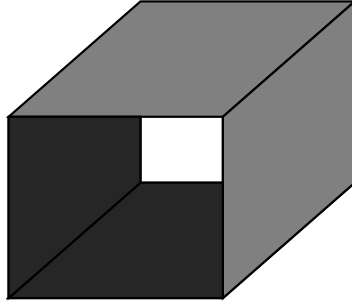


Figure 2. One of the three possible orientations of an elementary matchbox surface.

$$\begin{aligned} e\sigma &= \sigma, \quad e\tau = \tau, \quad e\eta = \eta \\ \sigma^2 &= \tau^2 = \eta^2 = e \\ \sigma\tau &= \eta, \quad \tau\eta = \sigma, \quad \eta\sigma = \tau \end{aligned} \quad (9)$$

with e representing the unshaded cube, which means the spins live in the fourth order Abelian group. For convenience in simulations the spins may also be considered as Ising (± 1) spins if we set $\eta_i = \sigma_i \tau_i$, which recasts the Hamiltonian into

$$H_{dual} = -\frac{1}{2} \sum_{\langle ij \rangle} \sigma_i \sigma_j - \frac{1}{2} \sum_{\langle ik \rangle} \tau_i \tau_k - \frac{1}{2} \sum_{\langle jk \rangle} \sigma_j \sigma_k \tau_j \tau_k, \quad (10)$$

which is recognizable as an anisotropically coupled Ashkin-Teller [10] model with equal couplings. Without the four-spin term this would simply be two uncoupled 1D Ising chains arranged in perpendicular directions and thus display no transition(s), but as we see below the coupling via the Ashkin-Teller energy term in the third direction gives non-trivial behaviour.

In the isotropically coupled case the ratio in equ.(10) corresponds to the increased symmetry point of the standard Ashkin-Teller model where the generic $\mathbb{Z}_2 \times \mathbb{Z}_2$ symmetry

is promoted to \mathbb{Z}_4 . This can be seen explicitly by rewriting the Hamiltonian in terms of the four double spins $S_i = (\pm 1, \pm 1)$ to give the 4-state Potts Hamiltonian

$$H_{dual, isotropic} = -\frac{1}{2} \sum_{\langle ij \rangle} (4\delta_{S_i, S_j} - 1) \quad (11)$$

where the sum now runs over all the edges orientations. 4-state Potts critical behaviour (i.e. a first order phase transition in 3D [11]) is thus found in the isotropic case.

In the remainder of the paper we consider the behaviour of the 3D dual Gonihedric Hamiltonian, as formulated in equ.(10) as an anisotropic Ashkin-Teller model, in its own right. We first look at the ground state structure of the model, highlighting the similarities with the plaquette action and in the light of this discuss coupled mean field equations on a cube. We then report on Monte Carlo simulations which are sufficient to confirm the nature of the phase transition and look at the effect of different cooling rates on the low temperature behaviour. The ground state, mean field and Monte-Carlo investigations all highlight the difficulty of formulating a standard magnetic order parameter, and we discuss the implications.

2. Ground State

In the isotropically coupled Ashkin-Teller model with equal positive couplings four equivalent magnetized ground states are possible, with the (σ, τ) spins taking the values (\pm, \pm) at every site, so only paramagnetic or ferromagnetic behaviour is seen for the individual σ and τ spins in this coupling regime. To investigate the ground state/zero-temperature structure of the dual Gonihedric model we use an approach which proved useful for the original undualized Gonihedric model and consider possible spin configurations on an elementary cube [2]. This is sufficiently large to capture non-trivial structure and the full ground state is then obtained by tiling the 3D cubic lattice with compatible single cube configurations.

The full lattice Hamiltonian may be written as a sum over the individual cube Hamiltonians h_C ,

$$h_c = -\frac{1}{8} \sum_{\langle i, j \rangle} \sigma_i \sigma_j - \frac{1}{8} \sum_{\langle i, k \rangle} \tau_i \tau_k - \frac{1}{8} \sum_{\langle j, k \rangle} \sigma_j \sigma_k \tau_j \tau_k, \quad (12)$$

where the additional symmetry factor of $\frac{1}{4}$ takes account of one edge being shared by four cubes. If a configuration of spins on a cube minimizes h_c the full lattice ground state energy density will simply be given by h_c .

Looking at the configurations in Fig. (3) immediately makes it clear that there is considerably more freedom for possible ground states in the anisotropically coupled Hamiltonian of equ.(10) than in the standard isotropic Ashkin-Teller model. In addition to the reference ferromagnetic ground states in Fig. (3a) it is possible to flip a single horizontal face of τ spins on the cube at zero energy cost as in Fig. (3b), or a vertical face of either σ (Fig. (3c)) or both σ and τ spins (Fig. (3d)) on the differently oriented vertical faces. Flipping *two* faces in the same orientation takes one between the different

possible ground states of the standard isotropic model, so it is the ability to flip a single face at zero energy cost which confers the extra freedom in the anisotropic model.

It is also possible to combine the differently oriented single face flips on the cube without increasing the energy of the configuration. Tiling the entire lattice with such configurations then shows that ground states may contain flipped planes of σ , τ or $\sigma\tau$ spins (depending on the orientation) with respect to reference purely ferromagnetic ground states. It is possible for two orientations of flipped spin planes to intersect pairwise along a line or for three differently oriented planes to intersect at a point. The distribution of flipped spin planes in a ground state is thus completely arbitrary.

The ground state degeneracy of the dual Gonihedric model is thus similar to that of the original plaquette Hamiltonian of equ. (5) where (possibly orthogonal, intersecting) planes of spins may also be flipped at zero energy cost. Intriguingly, this

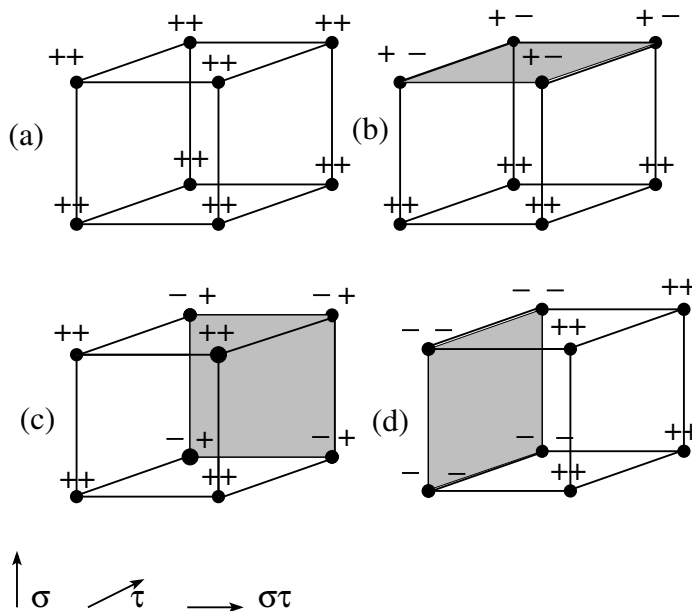


Figure 3. Some possible ground state spin configurations on a cube, the σ, τ values are shown at each site. The directions of the couplings in the Hamiltonian are indicated, as are the faces on which spins are flipped.

leads to the same difficulties in defining a suitable magnetic order parameter for the dual Hamiltonian as one faces with the plaquette Hamiltonian. Since arbitrary, and arbitrarily separated, spin planes may be flipped at zero energy cost a standard, or even a staggered magnetization, will generically be zero in such a state.

Of course, it is not guaranteed that ground state/zero-temperature degeneracies are maintained at finite temperature. Indeed, for the original Gonihedric model low temperature expansions by Pietig and Wegner [12] showed that when $\kappa \neq 0$, where it was still possible to flip arbitrary *parallel* spin planes to give a sandwich ground state, the ferromagnetic state had a lower free energy at finite temperature. The degeneracy did, however, persist at finite temperatures for the $\kappa = 0$ model. In the case of the dual Gonihedric model the Monte-Carlo simulations discussed below find

$\langle \sigma \rangle = \langle \tau \rangle = \langle \sigma \tau \rangle \sim 0$ in the low temperature phase, though there is a clear sign of a phase transition in the energetic observables and also the magnetic susceptibilities. This suggests that the flip symmetry persists at finite temperature throughout the low temperature phase.

3. Mean Field

In the mean field approximation an expression for the free energy is written by replacing the exact values of the spins with average site magnetizations and adding an entropy term. To take account of non-trivial structure in such a calculation one can again work at the level of the cubes, as for the ground state, and write down the coupled equations for the sixteen site magnetizations on the cube. The calculation of the mean field free energy in this manner is thus a direct elaboration of the method used to investigate the ground states. The total mean field free energy is written as a sum of the elementary cube free energies $\phi(m_C, n_C)$, given by

$$\begin{aligned} \beta \phi(m_C, n_C) = & -\frac{\beta}{8} \sum_{\langle i,j \rangle \subset C} m_i m_j - \frac{\beta}{8} \sum_{\langle i,k \rangle \subset C} n_i n_k - \frac{\beta}{8} \sum_{\langle j,k \rangle \subset C} m_j m_k n_j n_k \\ & + \frac{1}{16} \sum_{i \subset C} [(1 + m_i) \ln(1 + m_i) + (1 - m_i) \ln(1 - m_i)] \\ & + \frac{1}{16} \sum_{i \subset C} [(1 + n_i) \ln(1 + n_i) + (1 - n_i) \ln(1 - n_i)] \end{aligned} \quad (13)$$

where m_C, n_C is the set of magnetizations of the elementary cube with m_i, n_i the average site magnetizations for the σ_i and τ_i spins respectively. The log terms give the entropy for each of the types of spin. Minimizing this free energy gives a set of sixteen coupled mean-field equations

$$\begin{aligned} \frac{\partial \phi(m_C, n_C)}{\partial m_i} \quad (i=1\dots 8) & = 0 \\ \frac{\partial \phi(m_C, n_C)}{\partial n_i} \quad (i=1\dots 8) & = 0 \end{aligned} \quad (14)$$

(one for each corner of the cube and spin type) rather than the familiar single mean field equation for the standard nearest neighbour Ising action. The resulting equations are all of the form

$$\begin{aligned} m_1 & = \tanh[\beta(m_4 + m_2 n_1 n_2)] \\ & \vdots \\ m_8 & = \tanh[\beta(m_5 + m_7 n_7 n_8)] \\ & \vdots \\ n_1 & = \tanh[\beta(n_5 + n_2 m_1 m_2)] \\ & \vdots \\ n_8 & = \tanh[\beta(n_4 + n_7 m_7 m_8)] \end{aligned} \quad (15)$$

where we have labelled the magnetizations on a face of the cube counter-clockwise 1...4 and similarly for the opposing face 5...8, as shown in Fig. (4). If we solve these equations iteratively at different temperatures we arrive at zeroes for a paramagnetic phase or various combinations of ± 1 for the magnetized phases on the eight cube vertices.

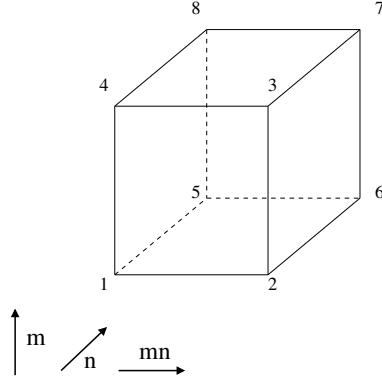


Figure 4. The labelling of sites used in writing the mean field equations for the cube. The directions of the mean field spin couplings in the Hamiltonian are again indicated.

A potential problem with an iterative scheme to solve the system of mean field equations

$$m_i^{(k+1)} = f_i[m^k, n^k], \quad n_i^{(k+1)} = f_i[m^k, n^k], \quad (16)$$

is that it might fail to converge if an eigenvalue of $\partial m_i^{(k+1)} / \partial m_j^k$ or $\partial n_i^{(k+1)} / \partial n_j^k$ is less than -1 [2]. This is easily remedied by modifying the equations to

$$\begin{aligned} m_i^{(k+1)} &= \frac{(f_i[m^k, n^k] + \alpha m_i^k)}{1 + \alpha} \\ n_i^{(k+1)} &= \frac{(f_i[m^k, n^k] + \alpha n_i^k)}{1 + \alpha} \end{aligned} \quad (17)$$

for a suitable α , and we have employed this here to ensure stability.

The mean field solution is then given by gluing together the elementary cubes consistently to tile the complete lattice, in the manner of the ground state discussion. In the limit $\beta \rightarrow \infty$ the mean field equations of equ.(16) become the system of equations

$$\begin{aligned} m_1 &= \text{sgn}[m_4 + m_2 n_1 n_2] \\ &\vdots \\ m_8 &= \text{sgn}[m_5 + m_7 n_7 n_8] \\ &\vdots \\ n_1 &= \text{sgn}[n_5 + n_2 m_1 m_2] \\ &\vdots \\ n_8 &= \text{sgn}[n_4 + n_7 m_7 m_8] \end{aligned} \quad (18)$$

which are, as they should be, compatible with the various ground state structures shown in Fig. (3). Solving the mean field equations numerically finds a (single) transition at $\beta \sim 0.83$ from a paramagnetic state to one of the possible ground states. If the iteration is seeded with spin values close to ± 1 one of the ferromagnetic states is picked.

It would be interesting to refine the mean field solution further by employing a cluster variational approximation, which essentially amounts to “improving” the entropy term and can be combined with Padé approximant methods to obtain quite accurate critical exponent estimates [13]. This has been done successfully for the original Gonihedric model [14], but we do not pursue this further here, turning instead to Monte Carlo simulations to sketch out the phase diagram of the model.

4. Some (Modest) Monte Carlo

For comparison purposes the phase diagram for positive couplings for an isotropically coupled Ashkin-Teller model is shown schematically in Fig.(5) where J_2 is the two-spin and J_4 is the four-spin coupling [10, 11]. Decreasing the temperature along the $J_2 = J_4$ line moves from a paramagnetic phase to a phase in which all of $\langle \sigma \rangle, \langle \tau \rangle$ and $\langle \sigma\tau \rangle$ (“polarization”) are non-zero, which is sometimes called the Baxter phase. The transition takes place at the four state Potts point and is thus first order, as we saw from a direct rewriting of the Hamiltonian in equ.(11). We are principally

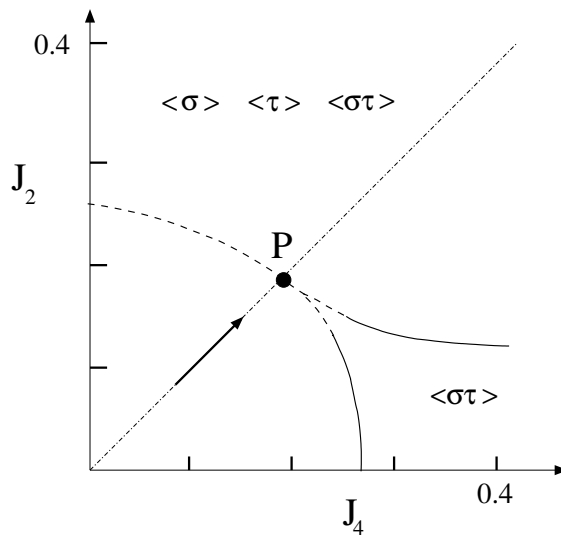


Figure 5. A schematic drawing of the phase diagram of the *isotropic* 3D Ashkin-Teller model for positive two-spin, J_2 , and four-spin, J_4 , couplings. The 4-state Potts point on the $J_2 = J_4$ line is marked as **P**. The indicated order parameters are non-zero in the phases shown on the diagram, and first order transition lines are shown as dashed lines, second order lines as solid. The paramagnetic phase surrounds the origin and the effect of decreasing the temperature along the $J_2 = J_4$ line is indicated by an arrow.

interested in determining the nature of the transition in the dual Gonihedric model here, for comparison with the phase diagram of the isotropic Ashkin-Teller model in

Fig. (5) rather than carrying out a high accuracy scaling analysis, so we use relatively modest lattice sizes and statistics in our simulations and employ a simple Metropolis update. Lattices of size $L = 10, 12, 14, 16, 18$ and 20 with periodic boundary conditions for both the σ and τ spins were simulated using both hot and cold starts at various temperatures. Following a suitable number of thermalization sweeps determined by the energy autocorrelation time, 10^7 measurement sweeps were carried out at each lattice size for each temperature simulated.

An estimate for the phase transition point of the original plaquette $\kappa = 0$ Gonihedric model is the value in [15] which takes account of the (effectively) fixed boundary conditions employed in the simulations there to fit to a suitable scaling form with the correct leading and subleading finite size corrections in such a case, $\beta_c(L) = \beta_c + a_1/L + a_2/L^2$. This found $\beta_c = 0.54757(63)$. Allowing for factors of 2 in the coupling definitions, an estimate for the dual transition temperature β_c^* is then given by the standard formula $\beta_c^* = -\ln[\tanh(\beta_c/2)] = 1.32$.

A plot of the energy is shown for various lattice sizes in Fig. (6) where there is clearly a sharp drop in the region of $\beta \sim 1.38$, somewhat higher than the estimate from the dual transition temperature. We can get a rough idea of the energy autocorrelation

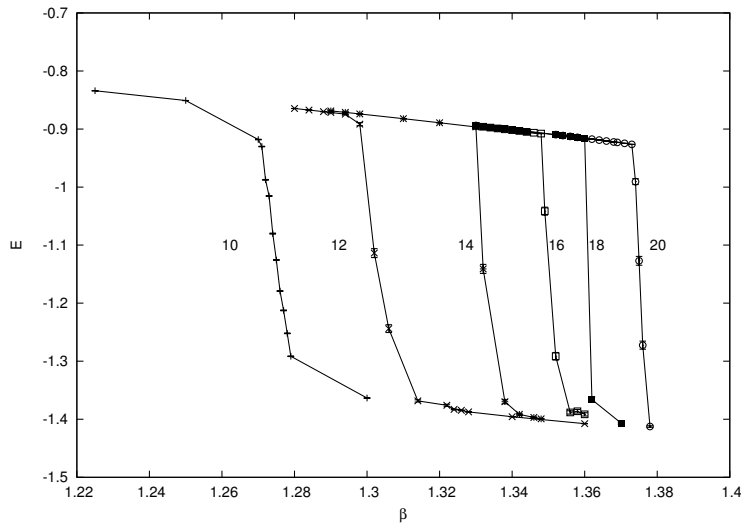


Figure 6. The energy for variously sized lattices ranging from 10^3 to 20^3 from left to right. The lines joining the data points are drawn to guide the eye and *hot* starts have been used in all the simulations.

time τ_e in the simulations by comparing the naive estimate for the variance (i.e. specific heat)

$$\epsilon_{naive}^2 = \sum_{j=1}^{n_m} \frac{(E_j - \langle E \rangle)^2}{n_m - 1} \quad (19)$$

where n_m is the number of measurements carried out, with a jack-knifed estimate using

binned data ϵ_{JK} . The two are related by

$$\epsilon_{JK} = \sqrt{\frac{2\tau_e}{n_m}} \epsilon_{naive}. \quad (20)$$

Away from the transition point we find $\tau_e \sim 1$ but large values of $\tau_e \sim 10^3$ appear in its vicinity.

There is no signal of the observed phase transition in any of the standard magnetic order parameters $\langle\sigma\rangle, \langle\tau\rangle$ and $\langle\sigma\tau\rangle$. This suggests that the degeneracy observed in the ground state features at finite temperatures as well. The susceptibility for both the individual σ and τ spins and the polarization $\sigma\tau$ is, however, non-zero and *does* show a signal at the phase transition point where, like the energy, it drops sharply. In Fig. (7) we plot the polarization susceptibility for $10^3 - 20^3$ lattices. The behaviour of the individual spin susceptibilities is very similar, with that for both the σ and τ spins showing a sharp drop from the high temperature phase to a much lower value at the same point.

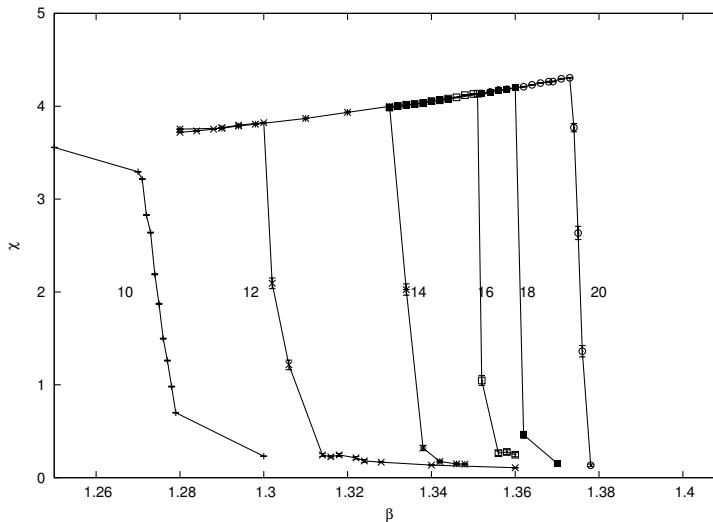


Figure 7. The polarization susceptibility, χ for a 10^3 to 20^3 lattices, showing a sharp drop near the pseudo-critical point in the region of $\beta = 1.375$ for the various lattice sizes. As for the energy in Fig. (6) the lines between the data points are drawn to guide the eye and hot starts have been used.

A good indicator of a first order transition is a bi-modal energy distribution at the transition point, so we also histogrammed the energy during the simulations. Looking at an energy histogram from a simulation sufficiently near the finite size pseudo-critical temperature should display a two-peak structure for a first order transition. A typical example for a 10^3 lattice close to its finite size pseudo-critical temperature at $\beta_c = 1.275$ is shown in Fig. (8), where we have histogrammed the 10^7 measurements of the energy which were carried out after each full lattice sweep of the σ and τ spins. The double peak structure expected of a first order transition is clearly visible. A direct consequence of

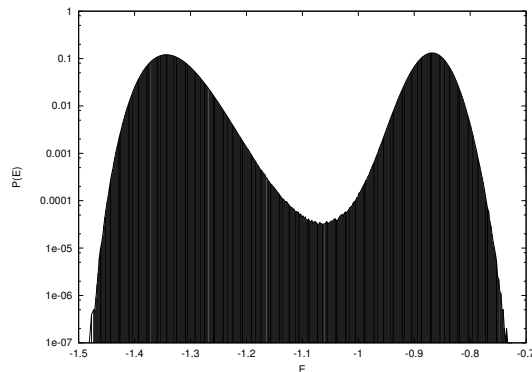


Figure 8. The energy histogram from a simulation with 10^7 sweeps on a 10^3 lattice near the finite size transition point (in this case $\beta = 1.275$). $P(E)$ is shown on a logarithmic scale.

the bi-modal energy distribution near criticality is a non-trivial limit for Binder’s energy cumulant. This is defined as

$$U_E = 1 - \frac{\langle E^4 \rangle}{3\langle E^2 \rangle^2} \tag{21}$$

which approaches $2/3$ at a second order transition point and a non-trivial limit at a first order point. We observe a non-trivial minimum value of U_E of $0.60(2)$, which varies little across the lattice sizes simulated.

Similarly, the β value of the minimum of U_E on an L^3 lattice, $\beta_{min}(L)$, is expected to scale as $\beta_{min}(L) = \beta_c - O(1/L^3)$ for a first order transition. If we plot the estimated minima positions for the various lattice sizes against $1/L^3$ we get a reasonable fit to this behaviour with a value of $\beta_c \sim 1.388(4)$ and a χ^2_{dof} of 1.34 when the smallest lattice size of 10^3 is dropped from the fits. The estimated value of β_c from this procedure is

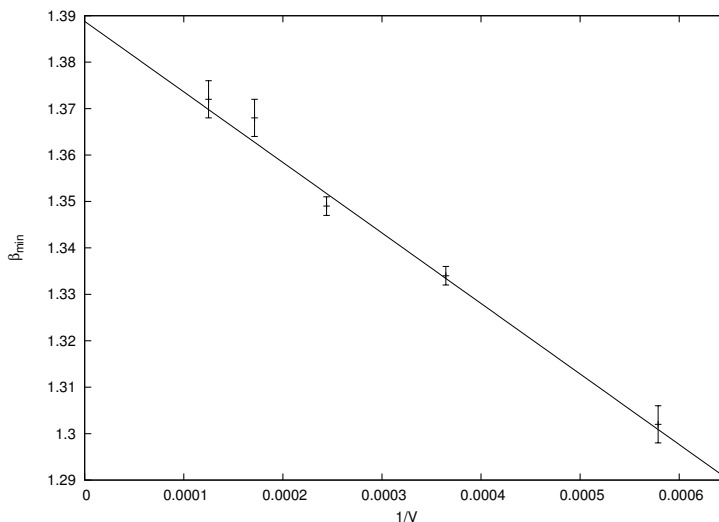


Figure 9. The scaling of the position of the minimum of the Binder energy cumulant against the inverse volume.

consistent with the behaviour of the energy and susceptibility jumps but, as we have already noted, it is somewhat higher than the dualized value calculated from the measurements in [15].

There is strong hysteresis around the transition point which may affect the accuracy of any such estimates. We show the result of using both ordered (cold) and disordered (hot) starting configurations for a 14^3 lattice in Fig. (10) with, in both cases, relaxation times of 10^4 sweeps followed by 10^7 measurement sweeps. This behaviour is again

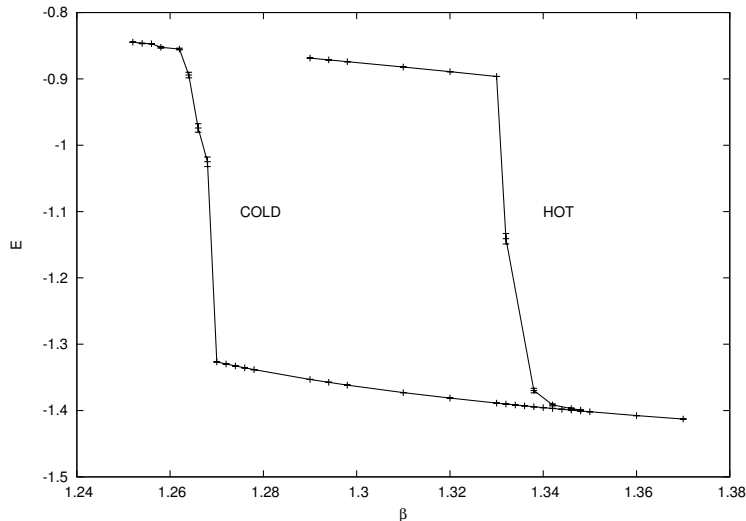


Figure 10. Measurements of the energy for hot and cold starts in the region of the transition point on a 14^3 lattice.

strikingly similar to that seen in the original plaquette Hamiltonian [5].

5. Some (Very Modest) Dynamics

An intriguing feature of the original $\kappa = 0$ Gonihedric model is its highly non-trivial non-equilibrium behaviour, including a region of metastability around its first order transition point and a dynamical transition which displays many glassy characteristics. We have seen that the dual Gonihedric model’s equilibrium phase diagram is similar to the original, so it is natural to inquire whether this similarity also holds for dynamical behaviour.

As a start in this direction, we cooled differently sized lattices at various rates from disordered (hot, “liquid”) starts in order to see if there was any evidence of the potentially glassy behaviour seen with the plaquette Hamiltonian. We cooled lattices of size 20^3 , 40^3 and 60^3 starting with a disordered configuration at a temperature of $T = 3$. From Figs. (11,12) it is clear that there is little difference between the 40^3 and 60^3 lattice results, while the 20^3 lattices may still be subject to stronger finite size effects. With regards to the numerical estimates of critical temperatures, this also suggests that the equilibrium simulations in the previous section may have been carried out on rather small lattices.

In Fig. (11) we can see that with a slow cooling rate of $\delta T = 0.00001$ per sweep, the systems still relax to a (ground) state with $E = -1.5$. The jump in the energy at the phase transition seen in the time series at $T \sim 0.72$ on the larger lattice sizes is consistent with the estimate of $\beta_c = 1.388(4)$ obtained from extrapolating the Binder cumulant values. Fig. (12), where a faster cooling rate of $\delta T = 0.001$ per sweep is employed, is

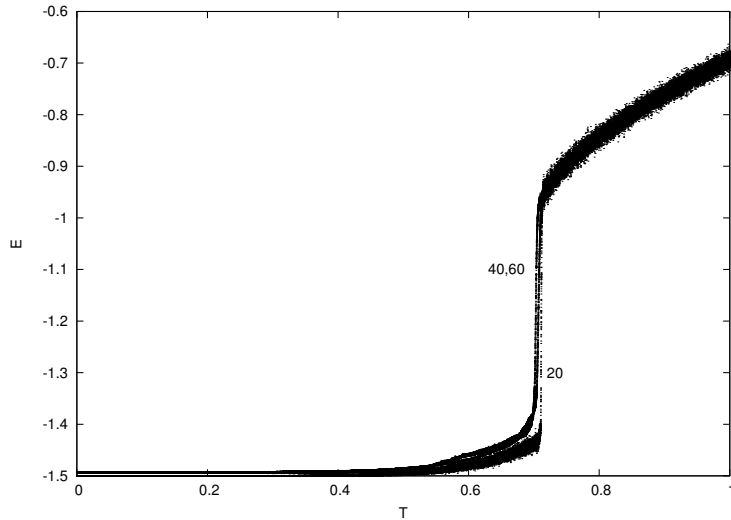


Figure 11. The time series of energy measurements obtained from cooling $20^3, 40^3$ and 60^3 lattices from a hot start at a rate of $\delta T = 0.00001$ per sweep.

perhaps more interesting. Once again there is little difference between the 40^3 and 60^3 lattices, but this time they do *not* relax to the ground state energy of $E = -1.5$, but are trapped at a higher value. Similar results in the plaquette model [5, 6] were taken

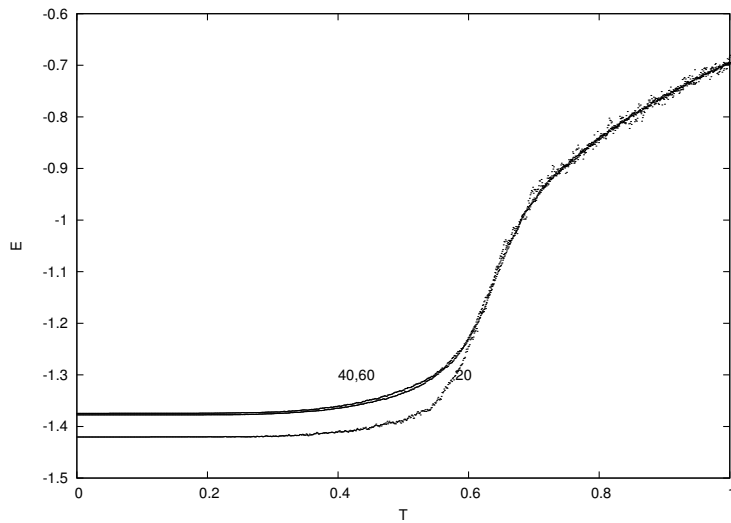


Figure 12. The time series of energy measurements obtained from cooling $20^3, 40^3$ and 60^3 lattices from a hot start at a rate of $\delta T = 0.001$ per sweep.

as an indicator of possible glassy behaviour, though there is evidence that what is seen

is an echo of a mean-field spinodal point [8] at which the supercooled high-temperature (“liquid”) phase becomes physically irrelevant.

6. Discussion

We have studied the dual of the $\kappa = 0$ Gonihedric Ising model in three dimensions, which may be formulated as an anisotropically coupled Ashkin-Teller model. We noted that this dual Gonihedric model displays clear signals of a first order transition, such as a bimodal energy histogram and a non-trivial limit for Binder’s energy cumulant (like the isotropically coupled equivalent), but it has a highly degenerate ground state (*un*-like the isotropically coupled equivalent).

The magnetic order parameters $\langle\sigma\rangle, \langle\tau\rangle, \langle\sigma\tau\rangle$ show no strong signal at the phase transition point which is, however, clearly visible in the energy and various susceptibilities as well as the Binder (energy) cumulant. The absence of conventional ferromagnetic order suggests that the degenerate ground state structure persists to finite temperatures, as is the case for the $\kappa = 0$ Gonihedric model. It would be an interesting exercise to carry out a low temperature expansion of the dual Hamiltonian to verify this by comparing the energy of the states with flipped spin planes to a ferromagnetic reference state in the manner of [12].

Another aspect which merits investigation is the crossover to the isotropic model, which has a much simpler ground state structure and known, simple order parameters for the low temperature phase(s). In any such endeavours the form of the anisotropic action suggests that it might be more amenable to a cluster simulation than the original plaquette action. The first order nature of the transition means that this would not confer such great advantages over local updates as in the case of continuous transitions, though cluster updates could be employed in conjunction with multihistogramming methods of various sorts for maximum numerical efficiency.

To investigate the non-equilibrium behaviour of the model, however, Metropolis (or other local) dynamics should be employed. We have made a start in this by conducting some cooling experiments which show that the phenomenology of the dual Hamiltonian appears to be remarkably similar to that of the original $\kappa = 0$ plaquette Hamiltonian. Under very slow cooling the ground state energy is achieved, but faster cooling appears to trap the system in a higher energy state. More extensive simulations along the lines of those conducted in [7,8] for the plaquette model and the the coupled two layer system (CTLS) would be useful to discern whether the “bubbling and coarsening” scenario posited there for the low temperature behaviour also applied in the case of the dual Gonihedric model, or whether more conventional coarsening dynamics was seen.

If the low temperature behaviour does, indeed, display (pseudo-)glassy characteristics it would also be useful to elucidate the nature of the self-induced frustration which is presumably causing it. For both the plaquette Gonihedric model and the CTLS multi-spin interactions appear to play a vital role. In view of the simplicity of the Hamiltonian, the dual Gonihedric model might also provide a further test case

in which to explore the approach of [16], which links dynamical, glassy behaviour in classical systems to quantum phase transitions.

7. Acknowledgements

The work of R. P. K. C. M. Ranasinghe was supported by a Commonwealth Academic Fellowship **LKCF-2010-11**. D. A. Johnston would like to thank W. Janke for useful discussions and comments.

- [1] R.V. Ambartzumian, G.S. Sukiasian, G. K. Savvidy and K.G. Savvidy, Phys. Lett. **B275** (1992) 99.
G. K. Savvidy and K.G. Savvidy, Int. J. Mod. Phys. **A8** (1993) 3393.
G. K. Savvidy and K.G. Savvidy, Mod. Phys. Lett. **A8** (1993) 2963.
J. Ambjørn, G.K. Savvidy and K.G. Savvidy, Nucl.Phys. **B486** (1997) 390.
- [2] A. Cappi, P. Colangelo, G. Gonella and A. Maritan, Nucl. Phys. **B370** (1992) 659.
- [3] G. K. Savvidy and F.J. Wegner, Nucl. Phys. **B413** (1994) 605.
G. K. Savvidy and K.G. Savvidy, Phys. Lett. **B324** (1994) 72.
G. K. Savvidy and K.G. Savvidy, Phys. Lett. **B337** (1994) 333.
G.K.Bathas, E.Floratos, G.K.Savvidy and K.G.Savvidy, Mod. Phys. Lett. **A10** (1995) 2695.
G. K. Savvidy and K.G. Savvidy, Mod. Phys. Lett. **A11** (1996) 1379.
G. Koutsoumbas, G. K. Savvidy and K. G. Savvidy, Phys.Lett. **B410** (1997) 241.
J.Ambjørn, G.Koutsoumbas, G.K.Savvidy, Europhys.Lett. **46** (1999) 319.
G.Koutsoumbas and G.K.Savvidy, Mod.Phys.Lett. **A17** (2002) 751.
D. Johnston and R.K.P.C. Malmimi, Phys. Lett. **B378** (1996) 87.
M. Baig, D. Espriu, D. Johnston and R.K.P.C. Malmimi, J. Phys. **A30** (1997) 405.
- [4] M. Baig, D. Espriu, D. Johnston and R.K.P.C. Malmimi, J. Phys. **A30** (1997) 7695.
- [5] A. Lipowski J. Phys. **A30** (1997) 7365.
- [6] A. Lipowski and D. Johnston, J. Phys. **A33** (2000) 4451.
A.Lipowski and D.Johnston, Phys.Rev. **E61** (2000) 6375.
A. Lipowski, D. Johnston and D. Espriu, Phys Rev. **E62** (2000) 3404.
- [7] P. Dimopoulos, D. Espriu, E. Jané and A. Prats, Phys. Rev. **E66** (2002) 056112.
- [8] M. Swift, H. Bokil, R. Travasso and A. Bray, Phys. Rev. **B62** (2000) 11494.
A. Cavagna, I. Giardina and T. S. Grigera, Europhys.Lett. **61** (2003) 74; J. Chem. Phys. **118** (2003) 6974.
S. Davatolhagh, D. Dariush and L. Separdar, Phys Rev. **E81** (2010) 031501.
- [9] G. K. Savvidy, K.G. Savvidy and F.J. Wegner, Nucl. Phys. **B443** (1995) 565.
G. K. Savvidy, K.G. Savvidy and P.G. Savvidy, Phys.Lett. **A221** (1996) 233.
- [10] J. Ashkin and E. Teller, Phys. Rev. **64** (1943) 178.
- [11] R. Ditzian, J.R. Banavar, G.S.Grest and L.P. Kadanoff, Phys. Rev. **B22** (1980) 2542.
G. Szukowski, G. Kamieniarz and G. Musiał Phys. Rev. **E77** (2008) 031124.
- [12] R. Pietig and F. Wegner, Nucl.Phys. **B466** (1996) 513.
R. Pietig and F. Wegner, Nucl.Phys. **B525** (1998) 549.

- [13] A. Pelizzola, Phys. Rev. **E49** (1994) R2503.
A. Pelizzola, Physica **A211** (1994) 107.
A. Pelizzola, J. Magn. Magn. Mat. **140-144** (1995) 1491.
A. Pelizzola, Phys. Rev. **E53** (1996) 5825.
- [14] E. Cirillo, G. Gonnella A. Pelizzola and D. Johnston, Phys. Lett. **A226** (1997) 59.
E. Cirillo, G. Gonnella and A. Pelizzola, Phys. Rev. **E 55** (1997) R17.
- [15] M. Baig, J. Clua, D.A. Johnston and R. Villanova, Phys. Lett. **B585** (2004) 180.
- [16] C. Castelnovo, C. Chamon and D. Sherrington, Phys. Rev. **B 81** (2010) 184303.